

Current Biology, Volume 26

Supplemental Information

**Effective Modulation of Male Aggression through
Lateral Septum to Medial Hypothalamus Projection**

Li Chin Wong, Li Wang, James A. D'Amour, Tomohiro Yumita, Genghe Chen, Takashi Yamaguchi, Brian C. Chang, Hannah Bernstein, Xuedi You, James E. Feng, Robert C. Froemke, and Dayu Lin

Supplemental Figures and Legends

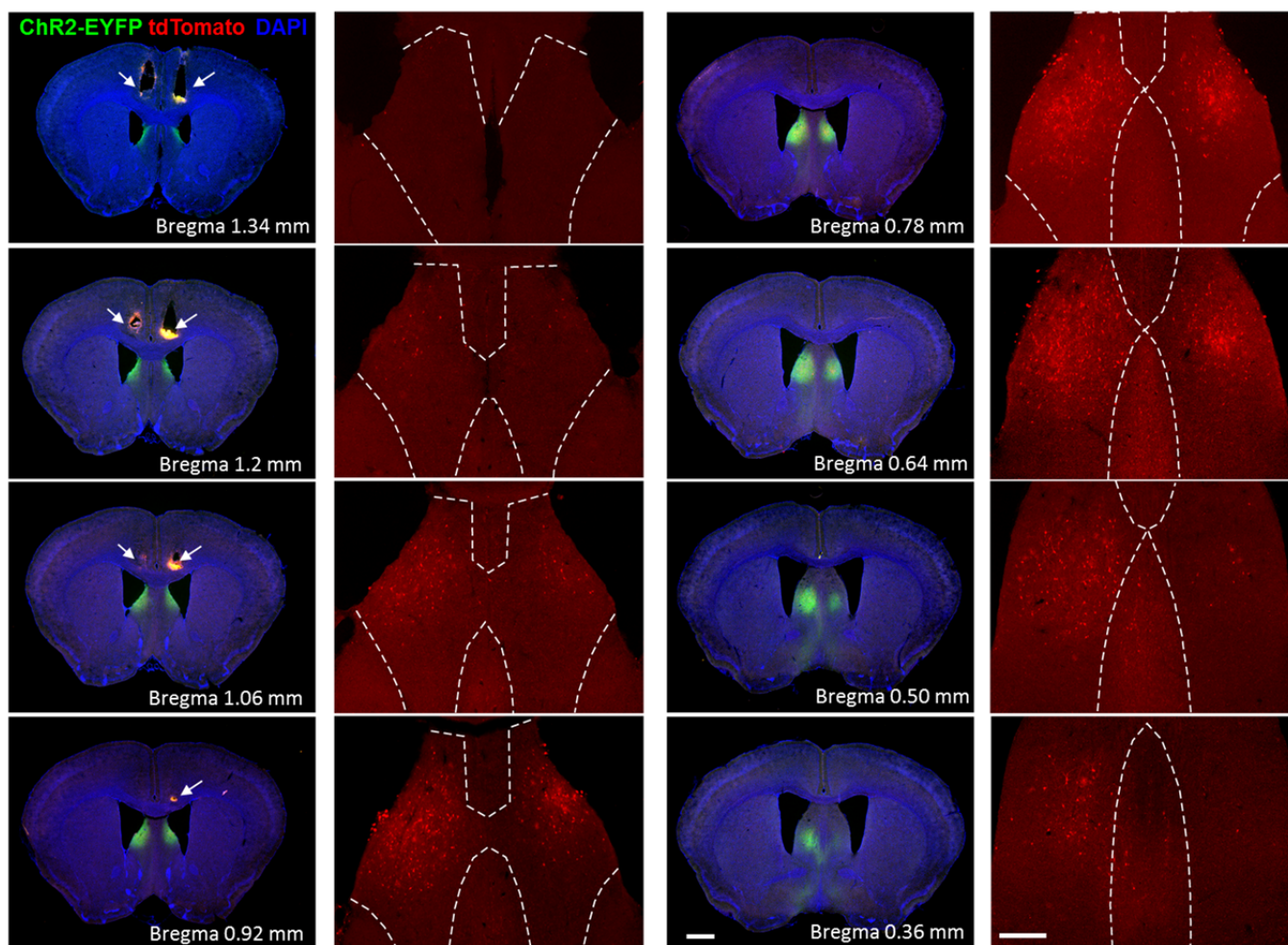


Figure S1: Complete expression pattern of ChR2-EYFP and tdTomato in the LS from a representative animal. Related to Figure 2. The first and third columns show macroscopic images of whole-brain sections from the anterior LS to the posterior LS. ChR2-EYFP (green) expression overlaps with tdTomato (red) expression. Blue: DAPI. White arrows indicate the tracks of the optic fibers. Scale bar for first and third columns: 1 mm. The second and fourth columns show the zoomed-in view of the expression of tdTomato in the LS. Dashes white lines mark the boundaries the LS. Scale bar for second and fourth column: 250 μ m.

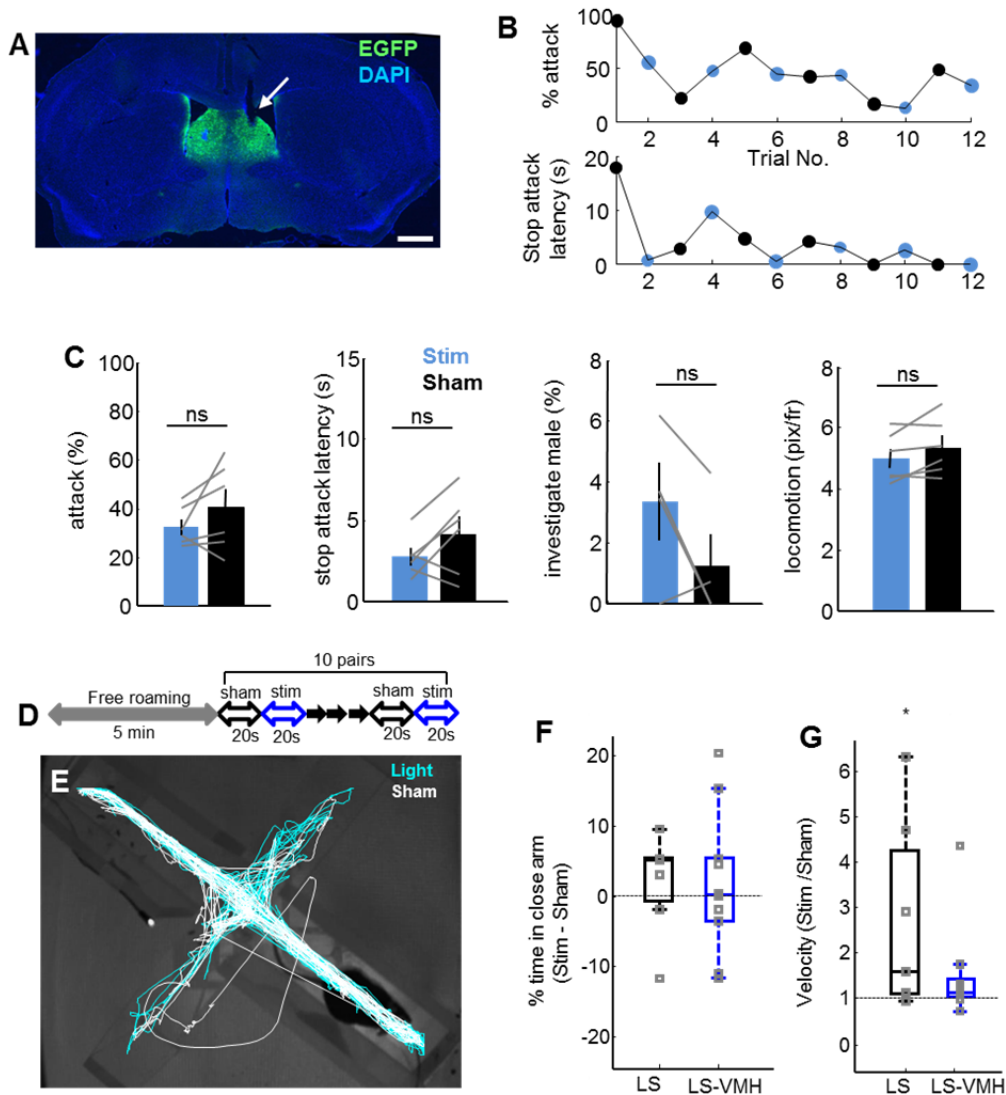


Figure S2: Control experiments for the LS and LS-VMH optogenetic stimulation. Related to Figures 2 and 3. (A) Coronal section showing virally mediated EGFP expression (green) in the LS and the cannula placement (arrow). Blue: DAPI. Scale bar: 0.5 mm. (B) Plots showing (top) the percentage of time that the animal spent on attacking, and (bottom) the latency to stop attack in an example session with interleaved stimulation trials (blue) and sham trials (black). (C) Bar plots showing no change in percentage time of attack, stop attack latency, percentage of time investigating male, and locomotion velocity during light stimulation (blue) and sham epochs (black). Error bars show \pm SEM. Each gray line represents one animal. $N = 6$. Paired t -test. all $p > 0.1$. (D) Time course of the elevated plus maze test. (E) Tracking results show movement of an animal during light (blue) and sham (white) periods in one session. (F) No difference in the percentage of time spent in the closed arm during stimulation and sham epochs across animals for LS stimulation group ($N = 7$) or LS-VMH stimulation group ($N = 9$). Error bars show \pm SEM. (G) Ratio of velocity during the light and sham periods increased dramatically in some animals during LS stimulation but not during LS-VMH stimulation. Error bars show \pm SEM. Signed-rank test. * $p < 0.05$. Horizontal dashed lines indicate expected value if light caused no behavioral change.

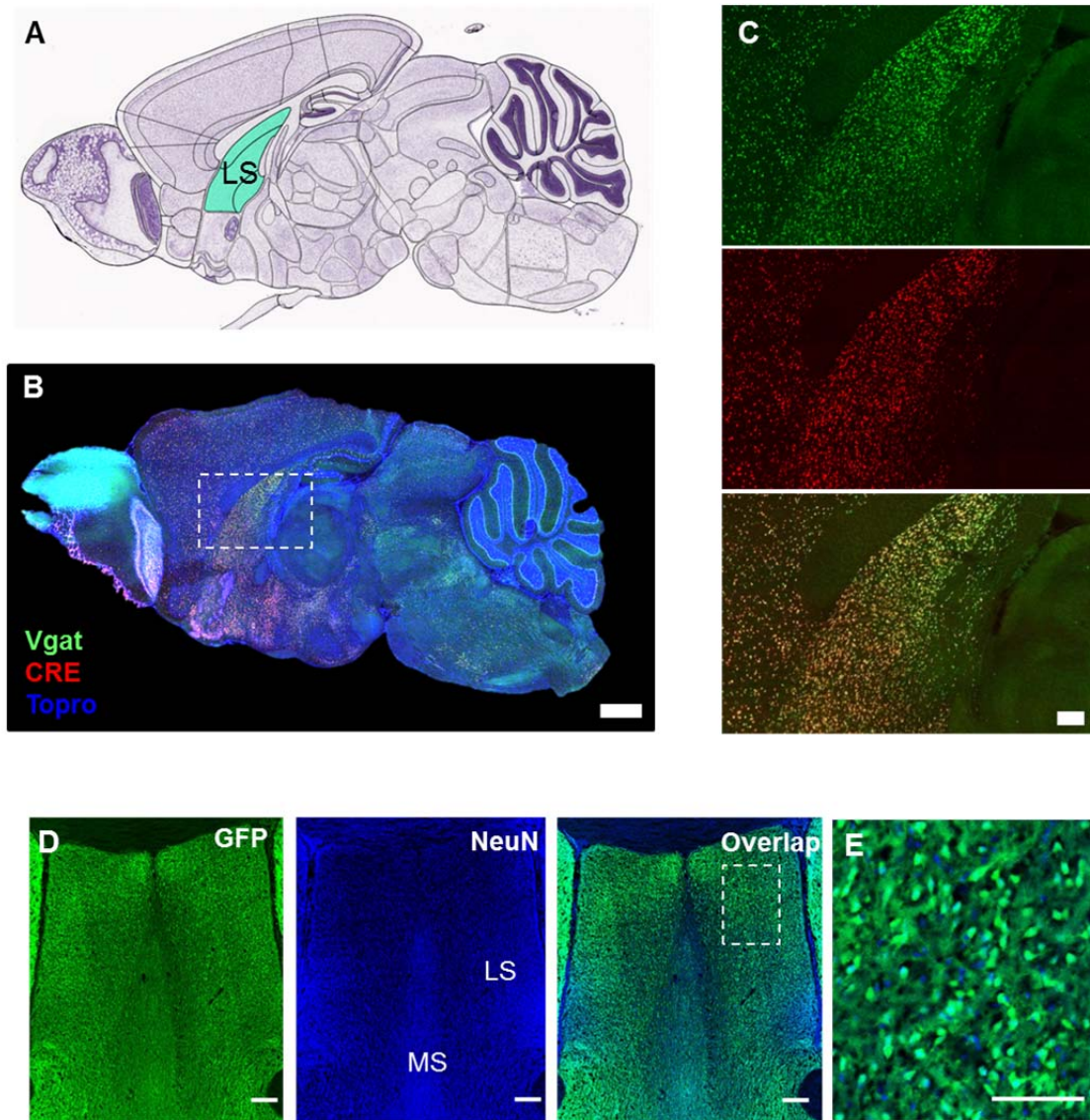


Figure S3: The LS comprises primarily GABAergic cells. Related to Figure 3. (A–C) Images adopted from <http://connectivity.brain-map.org/transgenic/experiment/304864567> showing double *in situ* visualization of VGAT (green) and CRE (red) in *Vgat*-ires-cre transgenic mouse. Scale bars in (B) and (C): 1 mm and 200 μ m, respectively. (D) Dense distribution of GFP positive cells (green) in the LS of *Vgat*-ires-cre \times RCE::loxP mice. Blue: NeuN. (E) Zoomed-in view of the box inset in (D). Scale bars in (D) and (E): 150 μ m and 75 μ m, respectively.

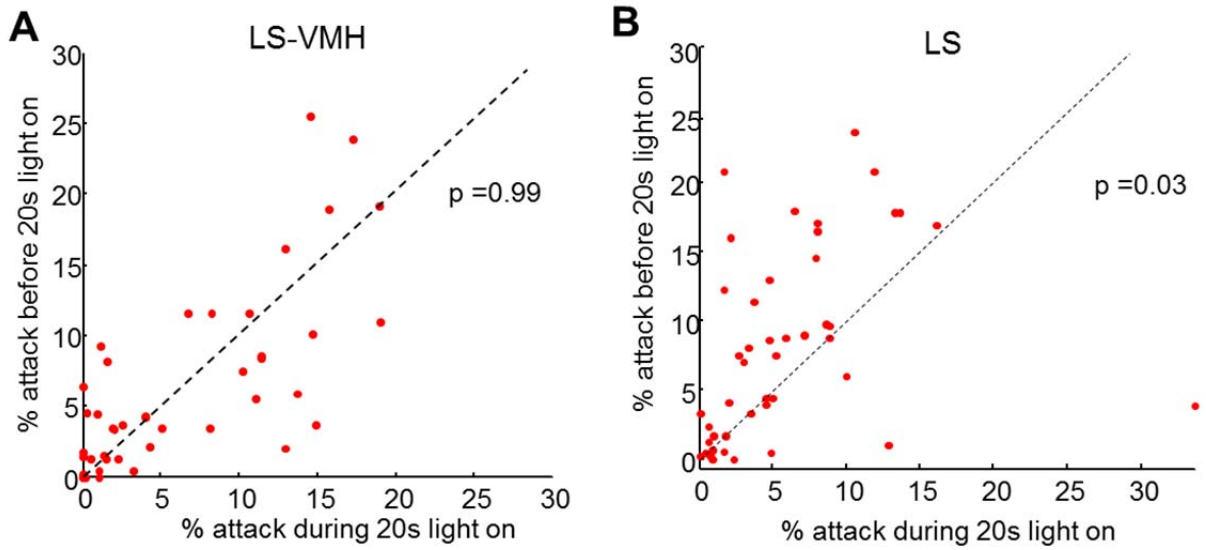


Figure S4: Aggressive behaviors during the optrode recording. Related to Figure 6. Light stimulation through the optrode at the VMHv1 (A) did not change attack time, but the light stimulation at the LS through the implanted optic fiber reduced the percentage time of attack (B) compared with the time-matched period prior to the stimulation. Paired *t*-test.

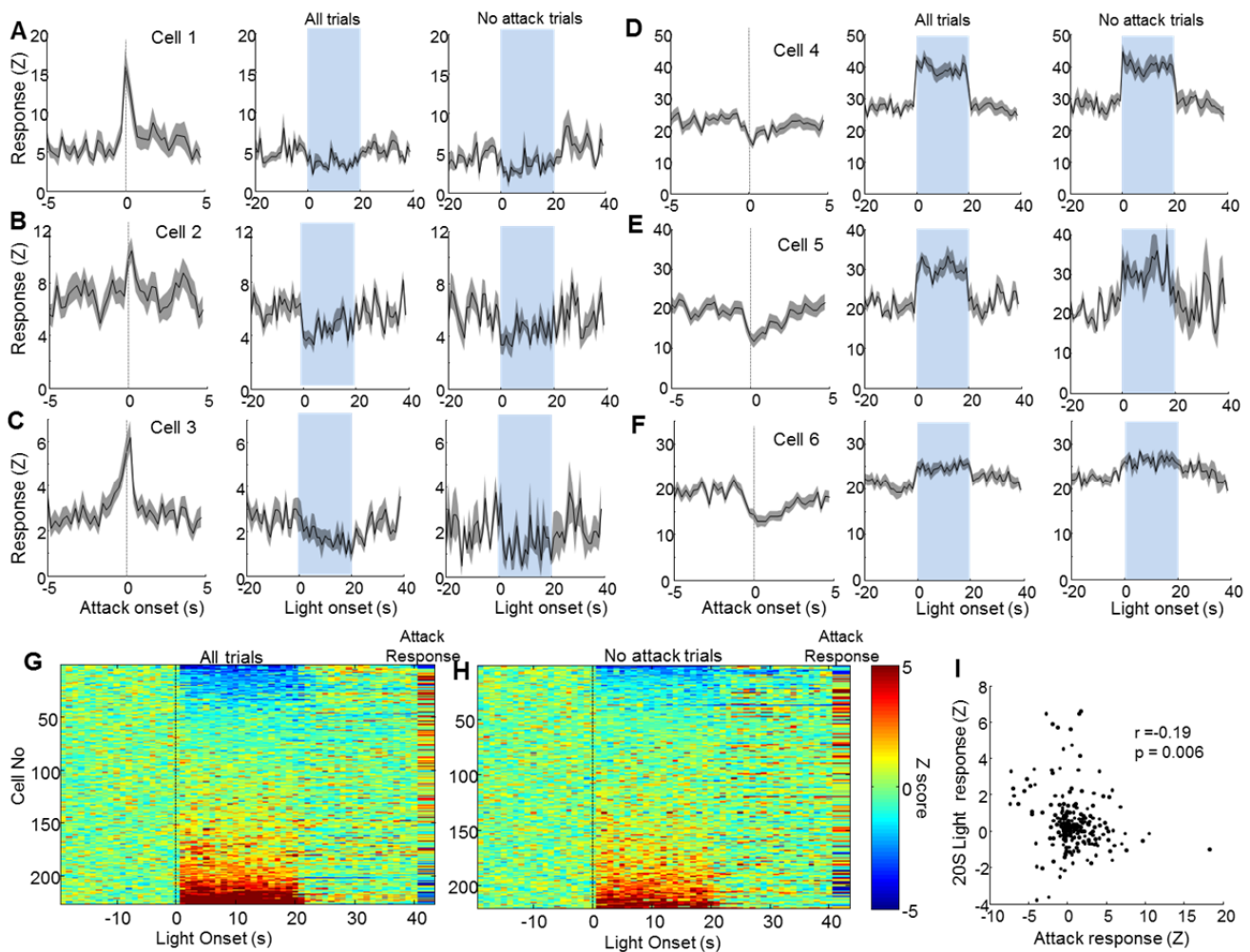


Figure S5: Stimulation of the LS changed the activity of attack-excited cells and attack-inhibited cells differentially. Related to Figure 7. (A–C) Three additional example cells that increased activity during attack (left column) but were inhibited during light stimulation (middle) even when only no-attack trials (from 20 s before stimulation to the end of stimulation) were considered (right column). Gray shading indicates \pm SEM. (D–F) Three additional examples of attack-inhibited but light-excited cells. Gray shading indicates \pm SEM. (G and H) Responses of all 224 cells aligned to the 20-s light pulse onset, sorted by averaged Z score during the whole light-on period. The right column of each map shows the attack response of each cell. G includes all trials. H includes only no-attack trials. (I) Scatter plot showing a significant negative correlation between attack response and the 20-s light-induced response during no-attack trials.

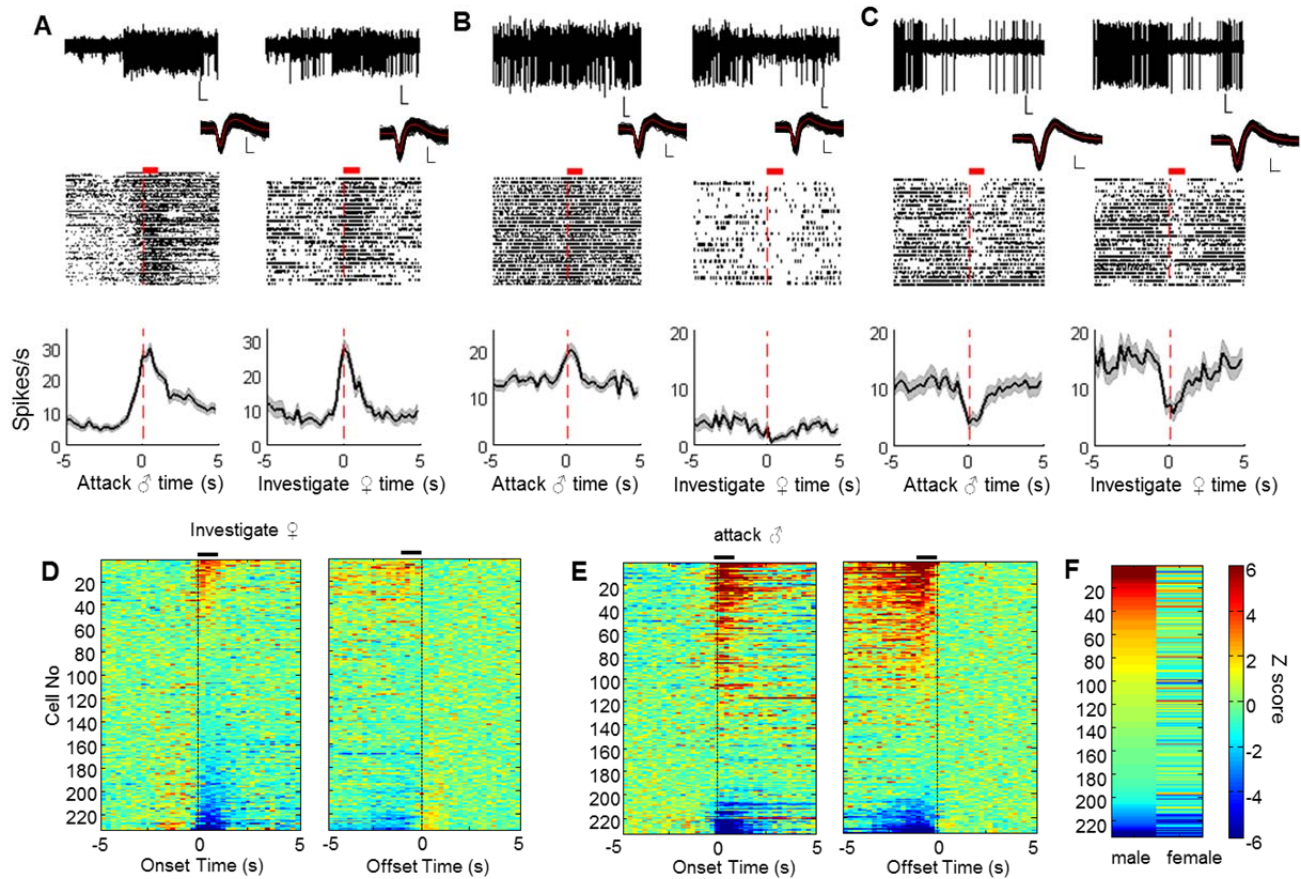


Figure S6. VMHvl cell responses to males and females. Related to Supplemental Experimental Procedures. (A–C) Responses of three representative cells during attacking males and investigating females. Images, from top to bottom, show the raw recording traces (vertical and horizontal scale bars: 100 μ V and 1s), waveforms throughout the recording (black) and their average (red) (vertical and horizontal scale bars: 100 μ V and 200 μ s), with raster plots aligned to behavioral onsets (red bars indicate the minimal behavioral duration) and corresponding PSTHs. Gray shading indicates \pm SEM. (D and E) Heat maps show the Z-score-normalized responses aligned to investigation of females (D) and attack of males (E). Cells are sorted based on their average response during the behaviors. Black bar indicates the minimal behavioral duration. (F) Heat map shows the average responses during attack of males (left) and investigation of females (right), sorted by male responses.

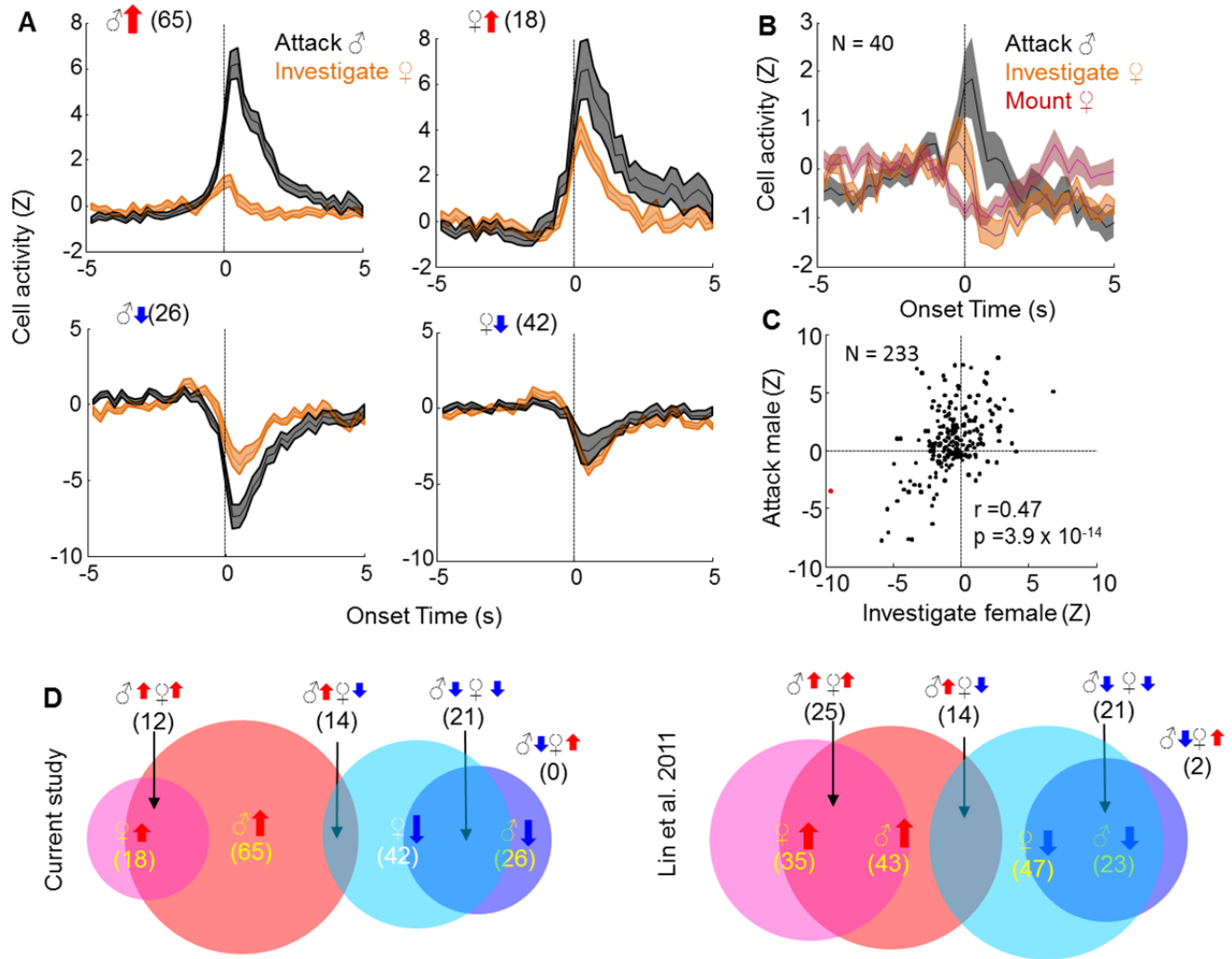


Figure S7: Relationship between VMHvl male-responsive and female-responsive units. Related to Supplemental Experimental Procedures. (A) The average Z-scored PSTHs aligned to attacking males (black) and investigating females (orange) of 65 male-excited cells, 18 female-excited cells, 26 male-inhibited cells and 42 female-inhibited cells. Note the female excited cells also show strong response during attacking males. Shades indicate \pm SEM. (B) The average Z-scored PSTH of 40 cells recorded with mounting events. Note the decreased activity during mounting. Shades indicate \pm SEM. (C) Across the population, responses of VMHvl cells during attacking male are highly correlated with the cell responses during investigating females. $r = 0.47$. $p = 3.9 \times 10^{-14}$. (D) Venn Diagrams showing the overlap between male-responsive and female-responsive cells in the current study and our previous study [S1].

Supplemental Experimental Procedures

Animals

Vgat-ires-Cre *Cre* and *Vglut2*-ires-Cre knock-in mice were generated by Dr. Lowell's group at Harvard University (now available at Jackson, stock No. 016962 and 016963) [S2]. Breeding colonies were maintained by mating *Vgat*-ires-Cre or *Vglut2*-ires-Cre mice with C57BL/6N (Charles River) at New York University Langone Medical Center (NYULMC). To reveal the CRE expression pattern, *Vgat*-ires-Cre mice were bred with GFP reporter mice (RCE:loxP line, provided by Dr. Fishell's lab at NYULMC) [S3]. All test animals were sexually experienced proven breeders. For optogenetic experiments, *Vgat*-ires-Cre and wild-type C57BL/6N mice (12–24 weeks, Charles River) were used; for *in vivo* electrophysiology, C57BL/6N mice were used. For *in vitro* electrophysiology, C57BL/6N and *Vglut2*-ires-Cre crossed with Ai6 mice (a ZsGreen reporter line from Jackson, stock no: 007906) were used. All test animals were single housed for at least 3 weeks before the test. Male intruders were selected randomly from a pool of (10–15 total animals) group-housed sexually inexperienced adult BALB/cmales (5 animals/cage, 10–30 weeks, Charles River). Female intruders were group-housed adult C57BL/6N females (5 animals/cage, 10–30 weeks, Charles River). Before each day of testing, females were screened for receptivity by placing each of them into the home cage of a sexually experienced single housed adult C57BL/6N male mouse for 5 minutes. If the female allowed the male to mount with no sign of rejection (running away, squeaking, or kicking), it was regarded as receptive and then used for the subsequent behavioral test. Mice were maintained on a reversed 12-hour light/dark cycle (dark cycle: noon to midnight) and given food and water *ad libitum*. All experiments were performed between 1 pm and 8 pm. All procedures were approved by the IACUC of NYULMC in compliance with the NIH guidelines for the care and use of laboratory animals.

Aggression screening

We performed a standard resident-intruder test to determine the aggression level of the animals prior to the functional manipulation experiments. During the screening, a group-housed BALB/cmale was introduced into the resident's cage for 10 minutes to allow free interaction once a day for 3 days. Animals that attacked for less than twice or less than 5 seconds in total on the last day of screening were determined as non-aggressive and used for the LS inactivation experiments. Animals that attacked for more than five times or more than 1 minute in total were determined as aggressive and used for optogenetic and electrophysiology experiments.

Pharmacological inactivation

For the LS inactivation, a double cannula (1.8 mm 26G thin wall stainless steel tubing, center to center distance = 1 mm, Plastics One) was implanted 0.5 mm above the LS (0.5 mm anterior-posterior (AP), 0.5 mm medial-lateral (ML), 1.8 mm dorsal-ventral (DV)). Two weeks after the surgery, 0.2–0.3 μ l of 0.33 mg/ml muscimol (Sigma) in saline was injected through the implanted cannula either using matching injectors (Plastics one) or a vertically mounted 0.5 μ l Neuros syringe (Hamilton) with a 31G beveled syringe needle. The injection speed was 0.1 μ l/min, and the final depth of injection was 2.5 mm (DV). For control experiments, the same volume of saline was injected. To reveal the location and extent of drug infusion, 0.2–0.3 μ l of 1.0 mg/ml fluorescent muscimol (M-23400, Life Technologies) in DMSO was injected 30 min before sacrificing the animal.

Two animals were excluded from the final analysis. In optogenetic experiments owing to the difficulty in obtaining histological data from them. The LS was inactivated by injecting 0.2–0.3 μ l of an 8% lidocaine (Sigma) and 0.1 μ M TTX (Tocris or R&D Systems) mixture in saline. After injection, animals were allowed to recover for 30 min before the behavioral test.

Stereotactic surgery and injection

For optogenetic manipulation, each wild-type mouse was injected bilaterally with a total volume of 0.2–0.5 μ l adeno-associated virus, which consisted of AAV2/1. EF1 α ::DIO.hChR2(H134R).EYFP (2×10^{12} PFU/ml, UNC Vector Core), AAV2/1 CMV::CRE (2×10^{12} PFU/ml, University of Iowa Gene Transfer Vector Core), and either AAV2/1 CMV::LacZ (titer 1×10^{12} PFU/ml, UNC Vector Core) or AAV2/1 CAG::DIO.tdTomato (2×10^{12} PFU/ml, Upenn Vector Core) into the LS (coordinates: 0.5 mm AP, 0.45 mm ML, 3.0 mm DV) at 10 nl/min using Nanoject injector (World Precision Instruments), followed by an additional 10 min before retraction. LacZ or tdTomato expression is mainly in the cell body and helps determine the primary infection site. Pilot experiments were performed using the same wild-type animals bilaterally injected with all the viruses except the LacZ or tdTomato cell body marking virus. Data from those pilot animals are qualitatively similar to those presented in the results but was not included in the final analysis. Data in Figure S2D–G were generated using those pilot animals. *Vgat*-ires-Cre mice were injected with 0.125–0.25 μ l AAV2/1 EF1 α ::DIO.hChR2(H134R).EYFP. Control animals were injected with 0.25 μ l of AAV2/1.CMV::PI.eGFP.WPRE.bGH (3×10^{12} PFU/ml). To stimulate the LS, a double cannula, the same as those used for the LS inactivation, was implanted 0.5 mm above LS. To stimulate the LS to VMHvl terminals, two 230- μ m multimode optic fibers with 1.25-mm ferrules were implanted 0.8 mm above the VMHvl area (–1.7 mm AP, 0.68 mm ML, 5.0 mm DV). Both cannula and optic fibers were secured to the skull with dental cement (Metabond, Parkell). For *in vivo* recording, a 16-channel optrode composed of sixteen 13- μ m tungsten microwires and one 105- μ m multimode optic fiber (Thorlabs) was attached to a moveable microdriver and inserted above the putative VMHvl area (initial implantation position: –1.7 mm AP, 0.68 mm ML, 5.2 mm DV) after virus injection into the LS and secured with bone screws and dental cement. The tip of the optic fiber was etched by dipping into hydrofluoric acid for 40 min [S4]. Recordings were done in a total of 20 animals. Analysis was done using the eight animals with electrode tracks centered in the VMHvl.

Optogenetic activation and behavioral tests

The behavior tests were done between 2–4 weeks for the LS direct stimulation and 4–8 weeks for the LS terminal stimulation after virus injection. To deliver light to the LS, two 230- μ m multimode optic fibers were inserted into the cannulas and secured with a matching cap (Plastics One). To deliver light to the VMH, two 230- μ m fibers (Thorlabs) with ferrules were connected to the implanted optic fiber ferrule assemblies with matching sleeves. The other end of the optic fiber was connected to a 100-mW, 473 nm blue laser (Shanghai Dream Lasers) controlled by computer programmed TTL pulses. All stimulations were done bilaterally.

In the aggression or mounting test, light-stimulation trials (20 ms, 20 Hz, 1–3 mW, 20 s) were interleaved with no light sham trials. Each test was completed after at least six pairs of sham and stimulation trials, or after 2

hours of testing. All trials were initiated when a spontaneous attack or mounting event was observed. All attack/mount/investigation events were manually annotated frame by frame. Behaviors of the same kind separated by less than 0.6 s (15 frames) were merged as one event. The latency to stop attack/mount was calculated from the time of light (sham or real) onset to the time when the ongoing attack/mount stopped. The percentage of time of attack/mount/investigation was calculated as the total time of the behavior divided by the total time of sham/real stimulation. The center location of the animal body was tracked using a custom written Matlab program [S5, S6]. Velocity was calculated as the Euclidean distance between the current frame and the previous frame. The number of sham/real stimulation trials varied across the animal due to behavioral variation. In our experiments, wild-type C57BL/6N animals were more aggressive than *Vgat-ires-Cre* animals and thus provided more trials per animal. Only animals tested with at least three pairs of light/sham stimulations were included in the analysis with one exception. In the LS inactivation experiment, one animal in LS stimulation with no drug condition contained only two pairs of stimulations. If data were determined to be normally distributed based on both the Jarque-Bera (JB) test and Lillie test, paired *t*-tests were used to test the difference between sham and real stimulation across the animals. If data were not normally distributed, the Wilcoxon signed-rank test was used. For optogenetic stimulation with the LS inactivation, results of all the groups were first confirmed to be normally distributed based on the JB and Lillie tests. Two-way ANOVA was then used to reveal the main causes of difference among groups, followed by a paired *t*-test between drug and no drug groups and a one-sample *t*-test to reveal behavioral changes under each stimulation/drug condition. For optogenetic stimulation with varying frequency, after confirming that data were normally distributed, repeated measure one-way ANOVA was used to examine group differences, followed by a paired *t*-test between each pair of stimulation conditions.

For the elevated plus maze test, after 5-min free exploration, animals received 10 interleaved sham and real stimulations (20 ms, 20 Hz, 1–3 mW, 20 s). Location of the animal was tracked to determine the time spent in each arm and instantaneous velocity.

***In vitro* slice electrophysiology and analysis**

Acute slices of the VMHvl were prepared from adult C57BL/6N mice that were used in the optogenetic experiments, and *Vglut2-ires-Cre* × *Ai6* mice injected with 0.25 μ l AAV2/1.EF1 α ::DIO.hChR2(H134R).EYFP (2×10^{12} PFU/ml, UNC Vector Core) in the LS. Animals were deeply anesthetized with a 1:1 ketamine/xylazine cocktail (100 mg/ml and 100 mg/ml, 0.1 ml) and decapitated. The brain was rapidly placed in ice-cold dissection buffer containing (in mM): 87 NaCl, 75 sucrose, 2 KCl, 1.25 NaH₂PO₄, 0.5 CaCl₂, 7 MgCl₂, 25 NaHCO₃, 1.3 ascorbic acid, and 10 dextrose, bubbled with 95%/5% O₂/CO₂ (pH 7.4). Slices (300–400 μ m thick) were prepared with a vibratome (Leica), placed in warm dissection buffer (33–35mM: 124 NaCl, 2.5 KCl, 1.5 MgSO₄, 1.25 NaH₂PO₄, 2.5 CaCl₂, and 26 NaHCO₃). Slices were kept at room temperature (22–24 °C) for at least 30 min before use. For experiments, slices were transferred to the recording chamber and perfused (2–2.5 ml/min) with oxygenated artificial cerebrospinal fluid (ACSF) at 33 °C.

Somatic whole-cell recordings were made from VMHvl neurons in voltage-clamp mode with a Multiclamp 700B amplifier (Molecular Devices). The VMH was identified either under infrared-differential interference contrast (IR-DIC) light microscopy (Olympus) as a dark oval shaped area close to the third ventricle or under the green fluorescent channel for slices from *Vglut2-ires-Cre* *e* × *Ai6* mice (Figures 5A–C). All recordings were made from an area close to the ventral boundary of the VMH. Patch pipettes (3–8 M Ω) were

filled with intracellular solution (in mM: 135 K-gluconate, 5 NaCl, 10 HEPES, 5 MgATP, 10 phosphocreatine, 0.3 GTP and 0.5% biocytin). At the end of each recording, the pipette was slowly moved away from the cell and lifted upward while applying weak positive pressure to retain the integrity of the soma.

The mean resting potential \pm standard deviation was -56 ± 6.5 mV, and the mean input resistance was 495.0 ± 300 M Ω , determined by monitoring cells with hyperpolarizing pulses (50 pA or 5 mV for 100 ms). Data were filtered at 2 kHz, digitized at 10 kHz, and analyzed with Clampfit 10 (Molecular Devices). The magnitude of the light-evoked IPSCs was measured as the peak values within a 5–10 ms window after light onset. The GABA_A receptor antagonist gabazine (1 μ M; Tocris Bioscience) or the GABA_B receptor antagonist CGP (1 μ M; Tocris Bioscience) were washed into the bath solution by diluting them into the perfused ACSF. For experiments in Figure 5F–H, we injected 500-ms incremental current steps (step size: 50 pA) ranging from 0 to 400 pA to evoke spiking in current-clamp. Each current step was repeated six times. In half of the trials, we simultaneously delivered 20 Hz 20 ms blue light pulses through the 40 \times objective. The first pulse occurred simultaneously with the onset current injection. For each cell, the average number of spikes under each current level was calculated and divided by the average spike number under the maximum current step. We then compared the normalized spike rate at each current level with and without the light across cells using Student's paired *t*-test. To investigate rebound spiking, we injected 500-ms incremental outward current steps (steps: -25 pA or -50 pA) ranging from -50 pA to -500 pA to hyperpolarize the cell. The initial sag was quantified as the peak hyperpolarization within the first 200 ms of the step minus the average membrane potential of the last 200 ms of the step. The number of rebound spikes was calculated as the number of spikes occurring within 300 ms after the current offset. We then calculated the average magnitude of the sag and the average number of rebound spikes across the current levels for each cell. The Pearson product-moment correlation coefficient between magnitude of the sag and the number of rebound spikes was then calculated across the cells.

Optrode recording

Methods for physiological recording in freely moving animals were as described [S1]. Briefly, 3 weeks after the virus injection, we connected the implanted optrode with a 16-channel headstage and a 105- μ m multimode optic fiber, and signals were streamed into a commercial acquisition system through a torqueless, feedback-controlled optrode commutator (Tucker Davis Technology) and band-pass-filtered between 100 and 5,000 Hz. During recordings, test animals remained in the home cage and were allowed to freely interact with an adult BALB/c male for 30 min and then with an adult C57BL/6 female for 10 min. To activate the LS-VMH pathway, blue light pulses (20 ms, 5 Hz for 20 s, 5–10 times) were delivered through the optrode in the presence of the male intruder. The final light intensity at the tip of the optrode was between 0.2 to 0.3 mW. To activate the LS, light (20 ms, 5 Hz for 20 s, 1–3 mW, 8–10 times) was delivered through the ipsilaterally implanted 230 μ m optic fiber in the LS. Digital infrared video recordings of animal behavior from both side and top view cameras were simultaneously recorded at 640 \times 480 pixel resolution at 25 frames per second (Streampix, Norpix). Video frame acquisition was triggered by a TTL pulse from the acquisition system to achieve synchronization between the video and the electrophysiological recording. Spikes were sorted using commercial software (OfflineSorter, Plexon) based on principal component analysis. Unit isolation was verified using autocorrelation histograms. To consider the recorded cell as a single unit, we imposed three criteria: 1) cells had to have a signal/noise ratio >3 ;

2) spike shape had to be stable throughout the recording; and 3) the percentage of spikes occurring with inter-spike intervals (ISIs) <3 ms (the typical refractory period for a neuron) in a continuous recording sequence had to be <0.1%. Among the 233 units recorded, 125 units met the criteria for single units, and the remaining 108 were regarded as multi-units. After the first recording, the implanted optrode was slowly moved down in 40- μ m increments until it reached 5.9–6.0 mm. The placement of the optrode was examined histologically.

Custom software written in Matlab (MathWorks) was used to facilitate frame-by-frame manual annotation of mouse behavior using side- and top-view videos (<http://vision.ucsd.edu/~pdollar/toolbox/doc/index.html>). Investigation was defined as nose-to-face, nose-to-body, or nose-to-urogenital contact. Attacks were defined by a suite of actions initiated by the resident towards the male intruder, which included lunges, bites, tumbling, and fast locomotion episodes in between such behaviors. For the inactivation experiments, videos were coded and annotated by the experimenter without knowing the manipulation condition. Videos for the optogenetic experiments were not coded, given that the stimulation condition (light or no light) was apparent from the videos.

Physiology analysis

All analyses were done using custom written software in Matlab. The response during each behavior was assessed with PSTHs. For each recorded unit, PSTHs were computed using 250-ms bins aligned to attack onset (onset PSTH) or offset (offset PSTH) and averaged across trials. PSTHs were then Z-score-transformed by subtracting the mean firing rate and dividing the standard deviation of the baseline firing (0–5 s after attack offset or –5 s to 0 s before investigating female onset, which contains relatively few social events). Population PSTH was calculated by averaging Z score transformed PSTHs of all relevant units. PSTHs for 20-ms light responses were computed using a 1-ms bin aligned to the light onset and Z score transformed using –10 ms to 0 ms preceding light onset as baseline period. PSTHs for 20-s overall light responses were computed using 1-s bin aligned to the first light pulse and Z score transformed using –20 s to 0 s preceding light onset as baseline period.

We calculated the averaged response during attack, female investigation, or light stimulation based on the Z scored PSTHs. For each unit, its attack response was calculated from the offset PSTH by averaging the values between –1 s to 0 s before the attack offset (250-ms bin). The female investigation response was calculated from the onset PTH by averaging the values between 0 to 1 s after the female investigation onset. Units with averaged Z score above 2 and below –2 were regarded as excited and inhibited units, respectively. The remaining units were regarded as not responsive. A cell's response to individual light pulses was calculated from the Z scored PSTHs aligned to the light onset. We calculated the averaged early light response to be between 8 ms and 15 ms (1-ms bin) after the light onset (Figure 6H), late light response between 0 and 20 ms after light offset (Figure 6I), and total light response between 8 ms after light onset and 20 ms after light offset (Figure 6J). The response during the total duration of the light was calculated as the averaged values between 0 to 20 s of the 20-s light PSTH of each unit. Pearson correlation coefficient was calculated to reveal dependence between behavioral responses and light responses across the population. The light responses of attack-excited, attack-inhibited, and attack-no-response units were compared using one-way ANOVA followed by *t*-test.

The heat maps were constructed by sorting the units based on their attack responses (Figures 6D and S6E–F) or female investigation response (Figure S6D), averaged activity between 8 ms after light onset to 20 ms after light offset (Figure 6G), averaged activity between 15 ms after light onset to 30 ms after light offset (Figure 7B) and averaged activity during the 20 s light-on period (Figures S5G and S5H).

Histology, Immunohistochemistry, and Microscopy

For histology verification of optogenetic experiments and *in vivo* recordings, standard immunohistochemistry procedures were followed to obtain and stain the 30- μ m brain sections for all mice. Mouse anti-NeuN (1:300, Millipore), rabbit anti- β -galactosidase (1:300, ICL lab), rabbit anti-GFP (1:300, Life Technologies), donkey anti-mouse Dylight 405 (1:300) and donkey anti-rabbit Dylight 488 antibodies (1:300, Jackson Immunoresearch), and DAPI (1:20,000, Life Technologies) were used. To label the recorded cells during slice recording, the slice was fixed in 4% paraformaldehyde for 1 hour, washed, and then soaked in 30% sucrose overnight. The slice was then stained with 1:500 Alexa 594 conjugated streptavidin (Invitrogen) overnight to label the recorded cells (more detailed procedure in [S7]).

To determine the placements of cannula, optic fiber, optrode and the injection sites of fluorescent muscimol, 1.6 \times or 2.5 \times fluorescent images were acquired. For GFP cell counting, 20 \times confocal images were obtained. For revealing the overlap between biocytin labeled cells and ZsGreen, Z-stack 40 \times confocal images were obtained. To quantify LacZ and tdTomato expressing cells in Figure 2C, 10 \times fluorescent images were acquired. For counting, we first selected regions of interest based on counterstaining and then manually counted cells in the blue and red channels using imageJ.

Electrophysiological responses of VMHvl cells towards females

During recording, a male BALB/c mouse was first introduced into the home cage of the recorded animal, which elicited quick attack. In the presence of the male intruder, we examined how stimulation of the LS-VMH and the LS evoked VMHvl cell responses. We then removed the male intruder, and 5 minutes later introduced a C57BL/6 female mouse for 10 min. The recorded animal quickly investigated the females and occasionally mounted the female during the recording period.

A total of 233 units were recorded from the putative VMHvl based on post-hoc histology. A variety of activity changes were observed during the attacks against males and the investigation of females (Figure S6). Approximately half of all recorded units (104/233) showed significant activity modulation (Z score > 2 or < -2) during attacks against males, investigation of females, or both. Generally, the activity change started as the recorded animal approached the intruder and reached maximum value at the onset of the behavior (Figures 6C and 6D, and S6A–C) and returned to the baseline at the offset of the behavior.

During attacks against males, we found that more than a quarter of units (65/233) significantly increased activity (average Z score > 2), and slightly more than 10% of the units (26/233) decreased activity (average Z score < -2). In comparison, during female investigation, less than 10% (18/233) of units increased activity and twice (average Z score > 2), as many units (42/233) were inhibited (average Z score < -2) (Figure S7D). Thus, whereas the dominant response of VMHvl cells to males is excitatory, the response to females is inhibitory. Among the 65 male-excited units, 12 units increased, 14 units decreased, and 39 units showed no significant change during female investigation (Figure S7D). Among the 18 female-excited units, 12 units significantly

increased firing during attacking male, and no unit was inhibited by exposure to another male (Figure S7D). Thus, female-excited cells are significantly enriched in the male-excited population (Fisher's exact test, $p < 0.001$). In support of this conclusion, we found a strong increase of activity in the female-excited population during attacks on male (Figure S7A). Since there are many more male-excited units than female-excited units, we found that as a population, male-excited units showed only minor increase during female investigation (Figure S7A). This result is qualitatively similar to our previous study showing that majority of male-excited and female-excited cells overlap [S1](Figure S7D).

For the inhibitory responses, the male-inhibited units and female-inhibited units also preferentially overlap (Fisher's exact test, $p < 0.001$). Among the 26 male-inhibited units and 42 female-inhibited units, 21 units are common (Figure S7D). Whereas male-inhibited units showed strong decrease during female investigation (Figure S7A, bottom left, orange line), female-inhibited units were clearly inhibited during attacking male (Figure S7A, bottom right, black line). This result is consistent with our previous report, showing that nearly all of the male-inhibited cells were inhibited during investigation of females (Figure 3e in [S1], Figure S7D). In the current study, animals showed limited sexual behavior during the 10-min testing period, and only 40 units were recorded during mounting. Among those 40 units, we observed an overall decreased activity during mounting (Figure S7B, red curve), slight increase during female investigation (Figure S7B, orange curve), and strong increase during attacks on males (Figure S7B, black curve).

Taken together, our data suggest that VMHvl cells are dominantly excited by males and inhibited by females. The female-excited VMHvl cells preferentially overlap with male-excited cells, and male-inhibited cells preferentially overlap with female-inhibited cells. Thus, across the population, there is a significant correlation between VMHvl cell response to female and male conspecifics (Figure S7C).

Supplemental References

1. Lin, D., Boyle, M.P., Dollar, P., Lee, H., Lein, E.S., Perona, P., and Anderson, D.J. (2011). Functional identification of an aggression locus in the mouse hypothalamus. *Nature* *470*, 221-226.
2. Vong, L., Ye, C., Yang, Z., Choi, B., Chua, S., Jr., and Lowell, B.B. (2011). Leptin action on GABAergic neurons prevents obesity and reduces inhibitory tone to POMC neurons. *Neuron* *71*, 142-154.
3. Sousa, V.H., Miyoshi, G., Hjerling-Leffler, J., Karayannis, T., and Fishell, G. (2009). Characterization of Nkx6-2-derived neocortical interneuron lineages. *Cereb Cortex* *19 Suppl 1*, i1-10.
4. Stark, E., Koos, T., and Buzsaki, G. (2012). Diode probes for spatiotemporal optical control of multiple neurons in freely moving animals. *Journal of Neurophysiology* *108*, 349-363.
5. Burgos-Artizzu, X.P., Dollár, P., Lin, D., Anderson, D.J., and Perona, P. (2012). Social Behavior Recognition in continuous videos. In *IEEE Conference on Computer Vision and Pattern Recognition* (Providence, Rhode Island).
6. Dollar, P., Welinder, P., and Perona, P. (2010). Cascaded Pose Regression. In *IEEE Conference on Computer Vision and Pattern Recognition*
7. Xu, H., Jeong, H.Y., Tremblay, R., and Rudy, B. (2013). Neocortical somatostatin-expressing GABAergic interneurons disinhibit the thalamorecipient layer 4. *Neuron* *77*, 155-167.